# Influence of Mode of Operation of the SSSC on the Small Disturbance and Transient Stability of a Radial Power System

Fawzi A. L. Jowder, *Member, IEEE*

***Abstract*—The static synchronous series compensator (SSSC), as a series compensator, has two ways of controlling the magnitude of the compensation, which are called 1) the *constant reactance mode* and 2) the *constant quadrature voltage mode*. In the *constant reactance mode*, the voltage, injected by SSSC, is proportional to the line current. In the constant quadrature voltage mode, the injected voltage of the SSSC is a constant that is in quadrature to the line current. This paper investigates the influence of the two modes on the damping power, synchronizing power, and transient stability limit of a radial power system. Eigenvalue analysis and digital simulation using HYPERSIM show that when the SSSC is in the *constant reactance mode* it provides higher damping power, synchronizing power, and transient stability limit than the case when the SSSC is in the *constant quadrature voltage mode*.**

***Index Terms*—Constant quadrature voltage mode, constant reactance mode, damping power, static synchronous series compensator (SSSC), synchronizing power, transient stability limit.**

## I. Introduction

SERIES capacitive compensation is used to offset the impedance of the transmission line such that the transmission line looks shorter. This improves the small disturbance and transient stability, which allows more power to be transmitted over the transmission line to load centers. The most economical way of providing series capacitive compensation is to use series dielectric capacitors, which have been widely installed all over the world. However, series capacitors can increase the potential for subsynchronous resonance (SSR) instability. For such situations, there are two series flexible ac transmission system (FACTS) devices that can also provide series capacitive compensation: 1) the thyristor controlled series capacitor (TCSC) [1], [2] and 2) the static synchronous series compensator (SSSC) [3]–[10]. The idea of TCSC [2] had evolved from the NGH damping filter in [1]. To date, several TCSCs are in operation [11]. The TCSC has been shown and used in practice to significantly improve the small disturbance and transient stability of power systems [11]–[18]. The SSSC is an electronic capacitor whose control system uses feedback control over voltage-sourced converters (VSCs) or current-sourced converters (CSCs) based on gate-turn-off-thyristors (GTOs) so that they produce a balanced set of voltages in quadrature with the transmission line current [3]–[10]. Although no stand-alone SSSC has been in service, it is the series converter of the unified power flow controller (UPFC) in the American Electric Power (AEP) system [19]. The SSSC, as a series compensator, has two modes of operation: 1) the constant reactance mode, in which the SSSC voltage is proportional to the line current, and 2) the constant quadrature voltage mode, in which the SSSC voltage is constant quadrature voltage independent of the line current. In [20], a damping controller with the SSSC in constant quadrature voltage mode has been designed to damp out power system oscillations. The constant reactance mode of the SSSC has been used in [21] to damp out the electromechanical oscillations.

Manuscript received June 28, 2004; revised November 8, 2004. Paper no. TPWRS-003530-2004.

F. A. L. Jowder is with the Department of Electrical and Electronic Engineering, University of Bahrain, Isa Town, Bahrain (e-mail: faljowder@eng.uob.bh).

Digital Object Identifier 10.1109/TPWRS.2005.846121

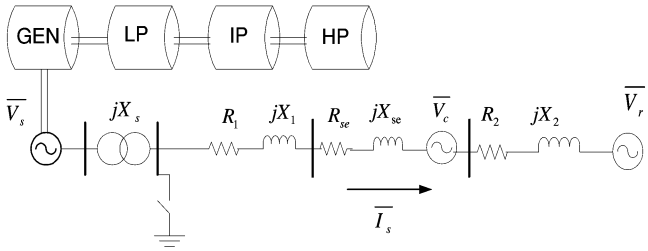


Fig. 1. Single line diagram of radial transmission system with SSSC compensation.

This paper applies eigenvalue analysis and digital simulations using HYPERSIM to study the influence of the two modes on the damping power, synchronizing power, and transient stability limit of an SSSC-compensated radial power system.

HYPERSIM, a digital simulator based on parallel computers, which Hydro-Quebec has developed for power system planning and operation, has been used to determine the transient stability limits. HYPERSIM has a comprehensive library of default options: detailed models of generators, field exciter systems, power system stabilizers, thermal turbines, governor systems, etc. [22]. The research has made use of the default models of a 1700-MVA thermal generator and associated equipment. The Appendix contains a list of parameters used in the eigenvalue analysis and the digital simulations.

## II. Power System Study Model

Fig. 1 shows the radial transmission system under study. The sending end voltage $\overline{V_s}$, representing a 1700-MVA thermal generator (GEN), is connected to the transmission line through a 20/315-kV transformer. In the per-unitization, the base values are $\mathrm{MVA_{base}} = 1700$, voltage $V_{\mathrm{Lbase}} = 315$ kV, and $Z_{\mathrm{base}} = 60\ \Omega$. The transformer is represented by the reactance $X_s$. The receiving end voltage $\overline{V_r}$ is an infinite bus. In the eigenvalue analysis, the 400-km transmission line is represented by circuit

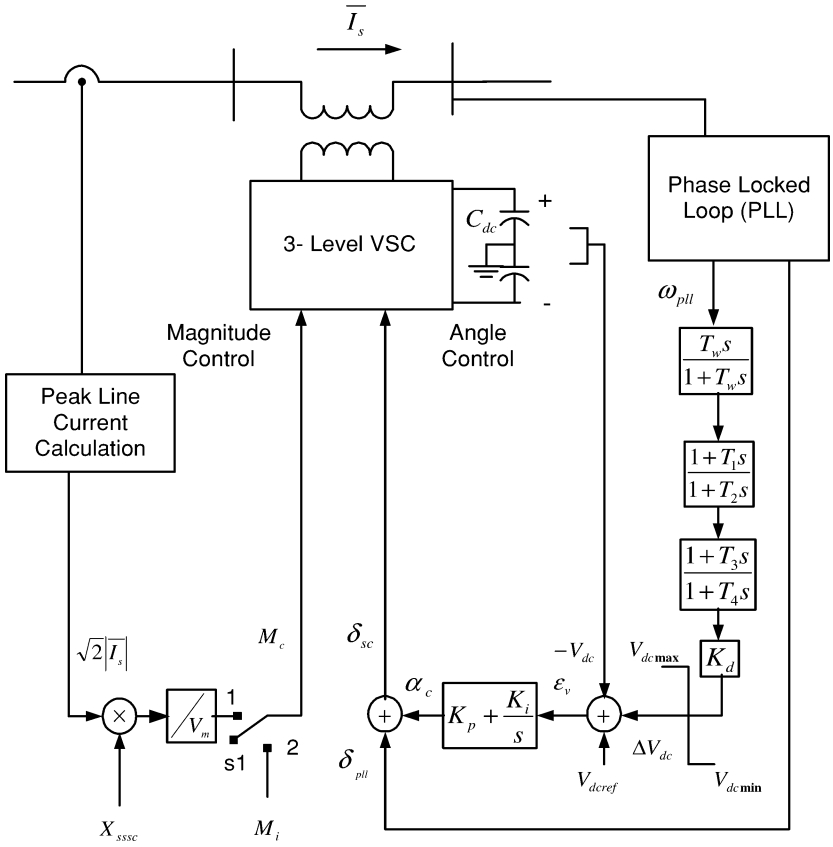


Fig. 2. Control of SSSC.

elements $R_{\rm ex}+jX_{\rm ex}=[R_1+R_2+j(X_1+X_2)]$. The per unit value of $X_{\rm ex}$ is given as 2.27 p.u. The SSSC is represented by an ideal voltage source $\overline{V_c}$ at the midpoint of the transmission line in Fig. 1. The equivalent resistance and inductive reactance of the series transformer are represented as $R_{\rm se}$ and $X_{\rm se}$.

The armature of the generator is described by Park's two axes model. The rotor comprises one field winding, one d-axis damper winding, and two q-axis damper windings. It has a field excitation system and a power system stabilizer system. The mechanical system consists of a three-stage steam turbine (HP, IP, LP) coupled to the generator. The inertia constants and the torsional spring constants are modeled. The boiler, the turbine, and the speed governor system are also modeled. The Appendix lists all the subsystems and the parameters used.

It has to be noted that in HYPERSIM, the transmission lines are modeled by telegraph equations (which is the method of Bergeron). In contrast, transmission lines are modeled as lumped L, R, and C circuit elements in the eigenvalue analysis.

## III. SSSC Controls

A block diagram of the SSSC is shown in Fig. 2. As the SSSC has been described in [3]–[9], only a brief outline is given here to make the paper self-sufficient. The equivalent voltage $\overline{V_c}$ in Fig. 1 represents the three-phase ac voltages produced by a three-level voltage-sourced converter (VSC) that are inserted in series in the transmission line by a transformer, as illustrated in Fig. 2. When the switch S1 in Fig. 2 is in position 1, the SSSC operates in the constant reactance mode ($\overline{V_c}=-jX_{\rm sssc}\overline{I_s}$), and when it is in position 2, the SSSC operates in constant quadrature voltage mode ($\overline{V_c}=-jV_q$).

### A. Magnitude Control of SSSC Voltage

By controlling the ON and OFF switching instants of the GTOs, the widths of the pulses are varied, and consequently, the magnitude $\overline{V_c}$ is controlled. In Fig. 2, when switch S1 is in position 1, the maximum line current $\sqrt{2}|\overline{I_s}|$, at which compensation is desired, is measured and multiplied by the equivalent $X_{\rm sssc}$ of the SSSC. The result is divided by the maximum series compensating voltage $V_m$ to yield $M_c=X_{\rm sssc}\sqrt{2}|\overline{I_s}|/V_m$, as the command to the magnitude control of the SSSC. With switch S1 in position 2, the command $M_c$ to the magnitude control of the SSSC is $M_i$.

### B. DC Voltage Regulation and Quadrature of Voltage to Current

In Fig. 2, the dc voltage error $\varepsilon_v=V_{\rm dcref}+\Delta V_{\rm dc}-V_{\rm dc}$, after passing the block with proportional gain $K_p$ and integral gain $K_i$, is applied in negative feedback to the phase angle control to null the error. Zero error implies that the real ac power, which enters the VSC, is just sufficient to replace converter losses to maintain the charge across the dc capacitor, a situation that is satisfied when $\overline{V_c}$ and $\overline{I_s}$ are almost $\pm 90^0$ apart. For capacitive compensation, $X_{\rm sssc}$ and $M_i$are positive, while for inductive compensation, $X_{\rm sssc}$ and $M_i$are negative.

### C. Damping Controller

The SSSC damping controller, to modulate the dc voltage of the VSC and consequently the voltage of the SSSC, is shown in Fig. 2. The line frequency of the voltages at the terminals of the SSSC is measured by a phase lock loop (PLL). The measured frequency $\omega_{\rm pll}$ is the input of the damping controller. The

input enters a washout filter (time constant $T_w$). Its output is passed through two cascaded lead compensators (time constants $T_1, T_2$ and $T_3, T_4$) and multiplied by a proportional gain $K_d$ to form the stabilizing signal $\Delta V_{\rm dc}$. $\Delta V_{\rm dc}$ is added to the set value $V_{\rm dcref}$. In the saturation block, the excursions of $\Delta V_{\rm dc}$ are limited above and below by $V_{\rm dc\,max}$ and $V_{\rm dc\,min}$. The parameters of the damping controller are designed with the help of eigenvalue analysis and repeated digital simulations.

### D. Relationship Between $X_{\rm sssc}$ and $M_i$

This section is devoted to ensuring that $X_{\rm sssc}$of the constant reactance mode and $M_i$ of the constant quadrature voltage mode are sized so that they yield the same degree of compensation. The degree of compensation $D_{\rm sssc}$ is defined as

$$D_{\rm sssc} = X_{\rm sssc}/X_{\rm ex}. \tag{1}$$

The degree of compensation $D_{\rm sssc}$ can be varied from $0 \le D_{\rm sssc} \le D_{\rm sssc\,max}$. At $D_{\rm sssc\,max}, X_{\rm sssc} = X_{\rm sssc\,max}$. The a-phase output of the VSC of the SSSC as viewed from the high voltage side of the transformer is

$$v_{\rm ca} = n\frac{V_{\rm dc}}{2} M_c \sin(\delta_{\rm sc}) \tag{2}$$

where

$M_c$ magnitude control command ($0 \le M_c \le 1$);
$V_{\rm dc}$ dc voltage;
$n$ transformer turns ratio;
$\delta_{\rm sc} = \delta_{\rm pll} + \alpha_c$ phase angle of the SSSC voltage.

When the switch S1 in Fig. 2 is in position 1

$$M_c = \frac{X_{\rm sssc}\sqrt{2}|\overline{I}_s|}{V_m}. \tag{3}$$

When the degree of compensation is $D_{\rm sssc\,max}$, corresponding to the compensating reactance $X_{\rm sssc\,max}$, and the line current reaches the maximum at which the compensation is still desired $|\overline{I}_{\rm srms}|$, the magnitude control command is $M_c = 1$. Therefore, from (3), the peak compensating voltage $V_m$ should be $\sqrt{2}|\overline{I}_{\rm srms}|X_{\rm sssc\,max}$. With $M_c = 1$, the VSC should produce the peak voltage

$$V_m = n\frac{V_{\rm dc}}{2}. \tag{4}$$

For $D_{\rm sssc\,max}, n(V_{\rm dc}/2) = \sqrt{2}|\overline{I}_{\rm srms}|X_{\rm sssc\,max}$.

Up to this point, the degree of compensation $D_{\rm sssc}$ has been directly related to $X_{\rm sssc}$ of the constant reactance mode. In the next paragraph, $D_{\rm sssc}$ will be related to $M_i$ of the constant quadrature voltage mode.

When switch S1 is in position 2, then the output of the VSC is the same as (2), except that $M_c = M_i$.

Therefore, according to (3)

$$M_i = \frac{\sqrt{2}|\overline{I}_s|X_{\rm sssc}}{V_m}. \tag{5}$$

When $M_i = 1$, this corresponds to the maximum compensation, i.e., the equivalent compensated reactance $X_{\rm sssc\,max}$. From (4), it follows that

$$1 = \frac{\sqrt{2}|\overline{I}_{\rm srms}|X_{\rm sssc\,max}}{V_m}. \tag{6}$$

Dividing (5) by (6)

$$M_i = \frac{X_{\rm sssc}}{X_{\rm sssc\,max}}. \tag{7}$$

Using (7), the same degree of compensation is obtained with both operating modes.

## IV. Eigenvalue Analysis

The linearized model of the system of Fig. 1, which is used to calculate the eigenvalues presented in this paper, is developed in [23]. The linearized model consists of the following four subsystems:

1) linearized model of generator with winding currents as state variables;
2) linearized model of mechanical system;
3) linearized models of excitation system and PSS.
4) linearized model of the SSSC, including the damping controller.

Reference [23] provides more details about the linearization procedure.

The damping power and the synchronizing power are related, respectively, to the real part and the imaginary part (frequency) of the eigenvalue that corresponds to the incremental change in the deviation of the rotor speed ($\Delta\omega$)and the deviation of the rotor angle ($\Delta\delta$)[24]. This eigenvalue is known as electromechanical mode (swing mode).

The eigenvalues of the system of Fig. 1 are calculated at different degrees of compensation $D_{\rm sssc}$ with SSSC operated in constant reactance mode and constant quadrature voltage mode. Only the results of the electromechanical mode are selected and presented in this paper. Other eigenvalues are stable and given in [23].

Figs. 3 and 4 show, respectively, the real part and the imaginary part (frequency) of the electromechanical mode as a function of the degree of compensation $D_{\rm sssc}$ with the SSSC operated in the constant reactance mode (curve 1) and the constant quadrature voltage mode (curve 2). The transmitted real power is $P = 0.5$ p.u. at a lagging power factor PF of 0.85.

It can be seen from Fig. 3 that below $D_{\rm sssc} = 0.5$, the constant reactance mode provides higher damping power. However, for $D_{\rm sssc} > 0.5$, the same mode provides lower damping power. For the same degree of compensation $D_{\rm sssc}$, the damping power can be controlled by increasing or decreasing damping controller gain $K_d$ in Fig. 2.

It can be depicted from Fig. 4 that when the SSSC is operated in the constant reactance mode, it provides higher synchronizing power than when it is operated in the constant quadrature voltage mode.

In order to increase the synchronizing power to a certain level, the degree of compensation required when the SSSC is in the constant reactance mode is smaller than the case when the SSSC is in constant quadrature voltage mode. In other words, the size of the SSSC is smaller.

Figs. 5 and 6 show the influence of the transmitted power $P$ on the damping power and the synchronizing power, respectively, for a degree of compensation $D_{\rm sssc} = 0.5$. The transmitted power is varied from $P = 0.3$ to 0.75 p.u. It can be seen from Figs. 5 and 6 that the damping power and synchronizing

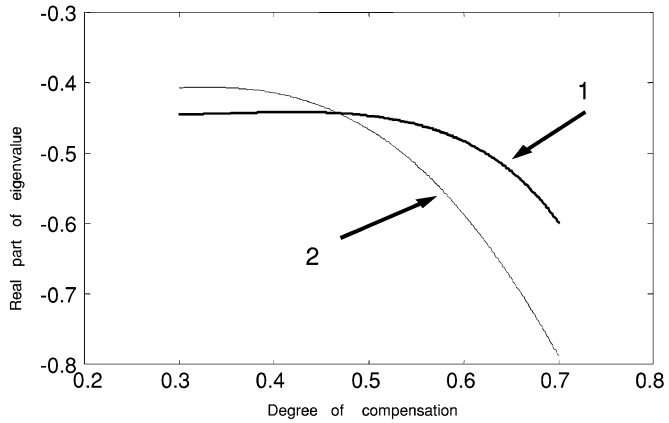


Fig. 3. Real part of electromechanical mode as a function of the $D_{\text{sssc}}$. ($P = 0.5$ p.u., PF $= 0.85$ lagging). 1) Constant reactance mode. 2) Constant quadrature voltage mode.

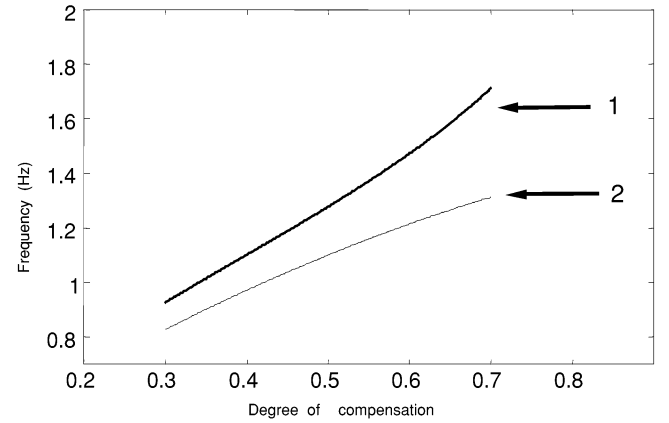


Fig. 4. Electromechanical frequency of oscillations (Hz) as a function of the $D_{\text{sssc}}$. ($P = 0.5$ p.u., PF $= 0.85$ lagging). 1) Constant reactance mode. 2) Constant quadrature voltage mode.

power decrease at a faster rate when the SSSC operated in constant quadrature voltage mode (curve 2) than the case in the constant reactance mode (curve 1).

Although Figs. 5 and 6 are presented for one degree of compensation, which is $D_{\text{sssc}} = 0.5$, the same conclusion can be drawn if the same test is performed for other degrees of compensation.

## V. Equal Area Criterion

The transmitted power in the radial power system of Fig. 1 with SSSC compensation operated in the constant reactance mode is [6], [9]

$$P_1 = \frac{|\overline{V_s}||\overline{V_r}|}{X_{\text{ex}} - X_{\text{sssc}}} \sin\delta \tag{8}$$

where

| | |
|---|---|
| $P_1$ | transmitted power with SSSC compensation in the constant reactance mode; |
| $X_{\text{ex}}$ | transmission line reactance; |
| $\lvert\overline{V_s}\rvert$, $\lvert\overline{V_r}\rvert$ | magnitude of the sending end and receiving end voltage; |
| $\delta$ | angle between $\overline{V_s}$ and $\overline{V_r}$; |
| $X_{\text{sssc}}$ | SSSC reactance (constant reactance mode). |

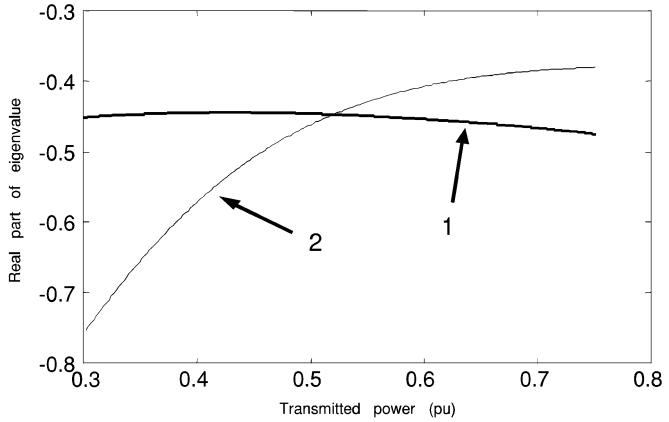


Fig. 5. Real part of electromechanical mode as a function of the $D_{\text{sssc}}$ ($D_{\text{sssc}} = 0.5$ p.u., PF $= 0.85$ lagging). 1) Constant reactance mode. 2) Constant quadrature voltage mode.

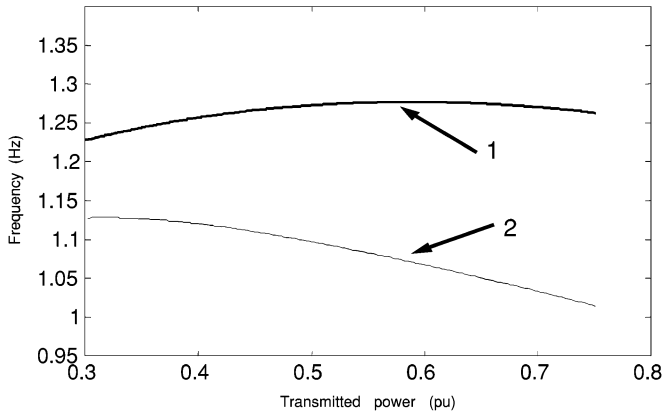


Fig. 6. Electromechanical frequency of oscillations (Hz) as a function of the transmitted power $P$ (p.u.). ($D_{\text{sssc}} = 0.5$ p.u., PF $= 0.85$ lagging). 1) Constant reactance mode. 2) Constant quadrature voltage mode.

The transmitted power in radial power system of Fig. 1 with SSSC compensation operated in the constant quadrature voltage mode is [4], [5]

$$P_2 = \frac{|\overline{V_s}||\overline{V_r}|}{X_{\text{ex}}} \sin\delta + \frac{|\overline{V_s}||jV_q|}{X_{\text{ex}}} \cos\frac{\delta}{2} \tag{9}$$

where $P_2$ is the transmitted power with SSSC compensation in the constant quadrature voltage mode, and $|jV_q|$ is the magnitude of the SSSC voltage (constant quadrature voltage mode).

Figs. 7 and 8 are equal area criterion diagrams of undergraduate textbooks to describe the transient stability limit. They have been drawn to illustrate the situations represented by (8) for the constant reactance mode and (9) for the constant quadrature voltage mode. In both cases, the degree of compensation is $D_{\text{sssc}} = 0.7$. For comparison, the power-angle curve for no compensation is shown by the curve labeled $D_{\text{sssc}} = 0.0$. The power-angle curves do not take into account the impact of the generator control systems (excitation system and speed governor system). It can be seen that the power-angle curve of Fig. 7 is different from Fig. 8. In Fig. 7, $\delta_0$ is the angle at which the three-phase fault is initiated, and $\delta_{\text{cr}}$ is the angle at which the fault is cleared. The difference between them is the clearing angle $\delta_c = \delta_{\text{cr}} - \delta_0$. The angle $\delta_m$ is equivalent to $\pi - \delta_0$. In Fig. 8, $\delta_0', \delta_{\text{cr}}'$, and $\delta_m'$ have the same definition as angles presented in Fig. 7.

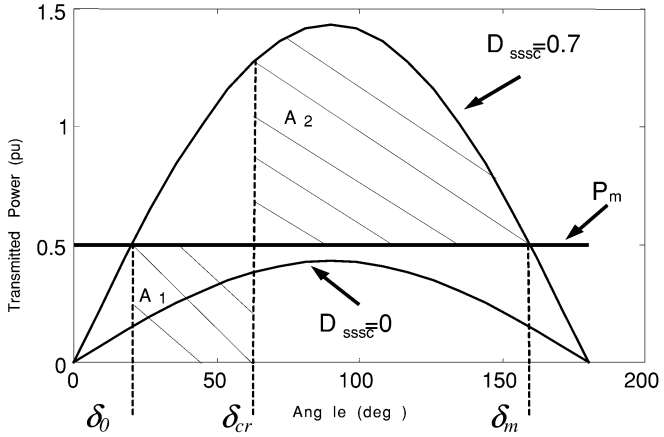


Fig. 7. Power-angle relation with the constant reactance mode. ($P_m = 0.5$ p.u. $|\overline{V_s}| = |\overline{V_r}| = 1, X_{\rm ex} = 2.3245, X_{\rm sssc0} = 1.627$ p.u.).

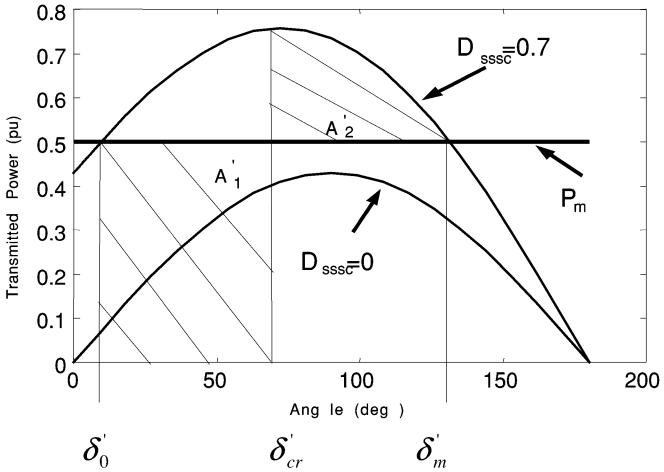


Fig. 8. Power-angle relation with the constant quadrature voltage mode. ($P_m = 0.5$ p.u. $|\overline{V_s}| = |\overline{V_r}| = 1, X_{\rm ex} = 2.3245, V_q = 1.0$ p.u.).

Areas $A_1$ and $A_1'$ present the kinetic energy picked up by the inertia $H$ during the fault. The kinetic energy released after clearing the fault is given as $A_2$ and $A_2'$. The equal-area criterion states that if $A_2 \geq A_1$, then the system is stable, and if $A_2 < A_1$, then system is unstable [24].

A simple numerical example is presented to illustrate the difference of the two modes *vis-à-vis* transient stability. Consider the following operating conditions:

$$\begin{aligned} P &= 0.5 \text{ p.u.} \\ |\overline{V_s}| &= |\overline{V_r}| = 1.0 \text{ p.u.} \\ X_{\rm ex} &= 2.3245 \text{ p.u.} \\ X_{\rm sssc} &= 1.6272 \text{ p.u. } (D_{\rm sssc} = 0.7), \quad V_q = 1.0 \text{ p.u.} \\ \delta_c &= 37.7^\circ \quad (\text{clearing time} = 100 \text{ ms}). \end{aligned}$$

Per unit values are calculated based on the MVA rating of the generator given in the Appendix. Using (4.40), (4.41), and (4.42) areas are given

$$\begin{aligned} A_1 &= 0.329. \text{ p.u.} \\ A_2 &= 1.5945 \text{ p.u.} \\ A_2' &= 0.4557. \text{ p.u.} \end{aligned}$$

Therefore, $A_2 > A_1$, and $A_2' > A_1$.

TABLE I
TRANSIENT STABILITY LIMITS AT DIFFERENT DEGREES OF COMPENSATION WITH SSSC IN CONSTANT REACTANCE MODE

| Degree of Compensation ($D_{sssc}$) | Transient Stability Limit | | |
|---|---|---|---|
| | Transmitted Power $P_{COMP}$ (pu) $P_{base}$=1700MW | Transmitted Power $P_{COMP}$ (MW) | Gain (pu) $G_{TSL}$ |
| 0 | 0.382 | 650 | 1.0 |
| 0.1 | 0.412 | 700 | 1.077 |
| 0.2 | 0.459 | 780 | 1.2 |
| 0.3 | 0.5 | 850 | 1.308 |
| 0.4 | 0.576 | 980 | 1.508 |
| 0.5 | 0.647 | 1100 | 1.692 |
| 0.6 | 0.765 | 1300 | 2.0 |
| 0.7 | 0.782 | 1330 | 2.046 |

TABLE II
TRANSIENT STABILITY LIMITS AT DIFFERENT DEGREES OF COMPENSATION WITH SSSC IN CONSTANT QUADRATURE VOLTAGE MODE

| Degree of Compensation ($D_{sssc}$) | Transient Stability Limit | | |
|---|---|---|---|
| | Transmitted Power $P_{COMP}$ (pu) $P_{base}$=1700MW | Transmitted Power $P_{COMP}$ (MW) | Gain (pu) $G_{TSL}$ |
| 0 | 0.382 | 650 | 1.0 |
| 0.1 | 0.412 | 700 | 1.077 |
| 0.2 | 0.441 | 750 | 1.154 |
| 0.3 | 0.482 | 820 | 1.262 |
| 0.4 | 0.524 | 890 | 1.369 |
| 0.5 | 0.563 | 957 | 1.472 |
| 0.6 | 0.594 | 1010 | 1.554 |
| 0.7 | 0.618 | 1050 | 1.615 |

Thus, the system is stable with both modes. However, $A_2$ is almost three times greater than $A_2'$, which indicates that the system transient stability limit can be increased to higher levels with the constant reactance mode. In contrast, $A_2'$ is greater but close to $A_1$; therefore, the transient stability limit is close to the transmitted power $P = 0.5$ p.u. at the specified $D_{\rm sssc}$.

## VI. TRANSIENT STABILITY LIMIT

The transient stability limit used in this paper is the maximum power that can be transmitted through the radial line of Fig. 1 without losing synchronism after a three-phase fault that cleared after 100 ms. The three-phase fault is applied at the high voltage side of the transformer of the generator. This is the standard fault that is used to produce the figures in this section. The transient stability limit is reached by repeated simulations with small increments in the transmitted power until synchronization is lost. The base line for comparison is the power at the transient stability limit $P_{\rm NC}$, when there is no compensation in the radial transmission line. When there is compensation by a degree of compensation ($D_{\rm sssc}$), the power of the transient stability limit is $P_{\rm COMP}$. The gain in power transmissibility is $G_{\rm TSL} = P_{\rm COMP}/P_{\rm NC}$.

Tables I and II summarize the power of the transient stability limits $P_{\rm COMP}$ and the gain in the power transmissibility $G_{\rm TSL}$ for different degrees of compensation ($D_{\rm sssc}$), which are chosen randomly, with SSSC operated in the constant reactance mode

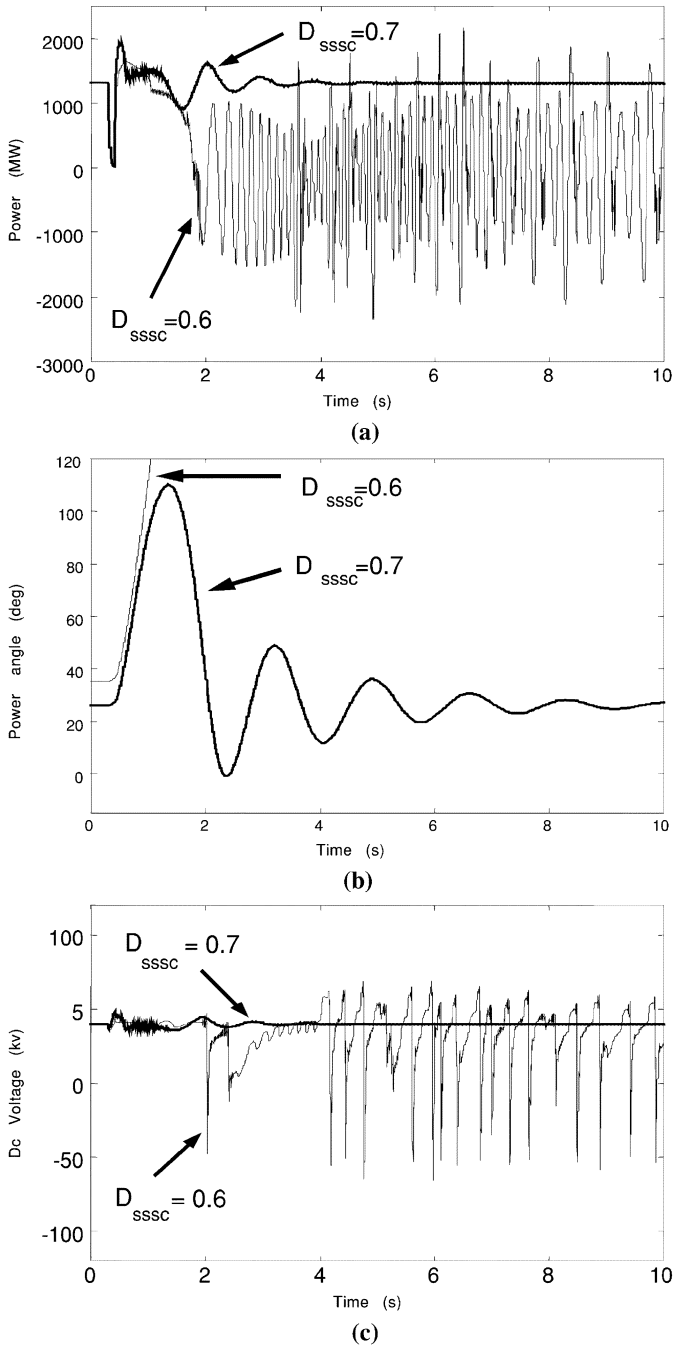


Fig. 9. System response after a three-phase fault for degree of compensation of $D_{\text{sssc}} = 0.7$ and $0.6$ p.u. (constant reactance mode). (a) Transmitted power (p.u.). (b) Power angle (degrees). (c) dc voltage (kv).

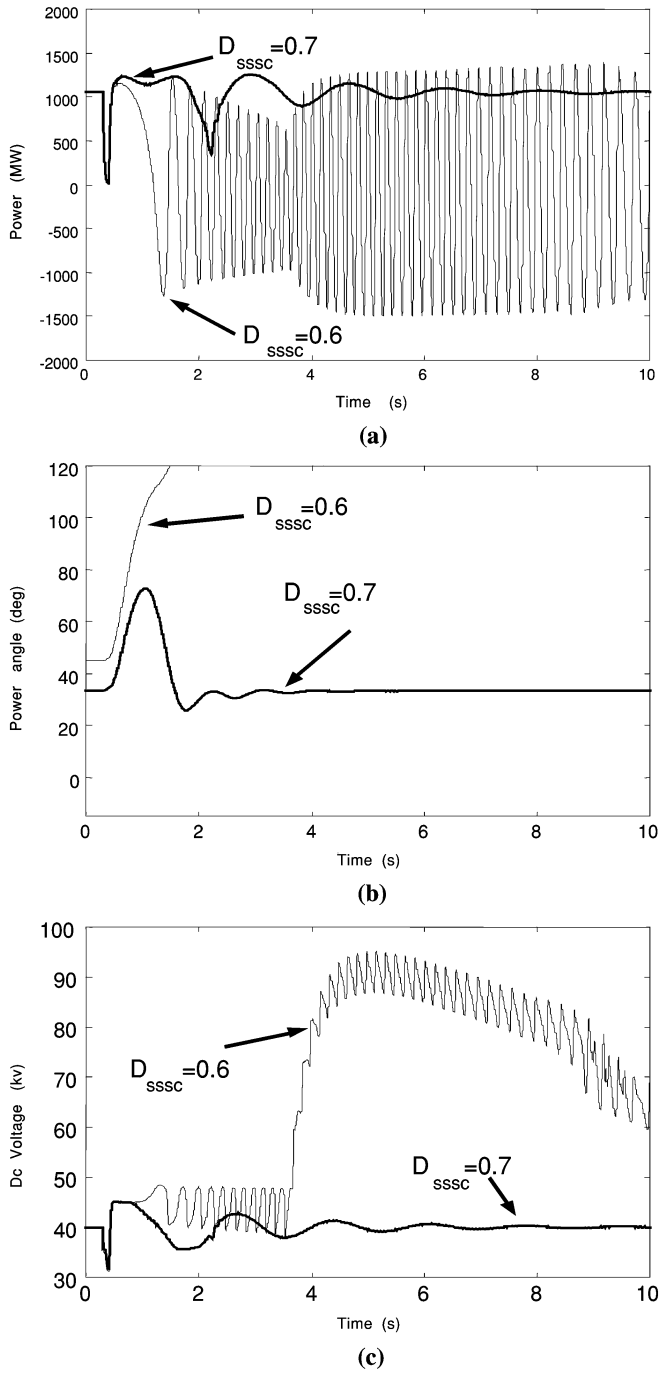


Fig. 10. System response after a three-phase fault for degree of compensation of $D_{\text{sssc}} = 0.7$ and $0.6$ p.u. (constant quadrature voltage mode). (a) Transmitted power (p.u.). (b) Power angle (degrees). (c) dc voltage (kv).

and the constant quadrature voltage mode, respectively. With the former mode, a gain of $G_{\text{TSL}} = 2.046$ is obtained with $D_{\text{sssc}} = 0.7$, while with the latter, $G_{\text{TSL}} = 1.615$.

A sample of the simulations in the transient stability tests, which establish that the transmissible power is 1330 MW for $D_{\text{sssc}} = 0.7$ when the SSSC in the constant reactance mode, is presented in Fig. 9. The standard three-phase fault is used. The plots in (a), (b), and (c) are, respectively, the instantaneous transmitted real power $P$ (MW), the power angle (degrees), and dc voltage (kV). Fig. 9(b) shows that for $P = 1330$ MW, after the clearance of the fault, the generator remains in synchronism for $D_{\text{sssc}} = 0.7$ p.u. but not for $D_{\text{sssc}} = 0.6$ p.u.

Fig. 10 shows a sample of the simulations in the transient stability tests, which illustrates that the transmissible power is 1050 MW for $D_{\text{sssc}} = 0.7$ in case of the constant quadrature voltage mode. Similar to Fig. 9, the plots in (a), (b), and (c) are, respectively, the instantaneous transmitted real power $P$ (MW), the power angle (degrees), and dc voltage (kV). Fig. 10(b) shows that for $P = 1050$ MW, after clearing the generator remains in synchronism for $D_{\text{sssc}} = 0.7$ p.u. but not for $D_{\text{sssc}} = 0.6$ p.u.

Fig. 11 presents a comparison between the two modes. Fig. 11(a) and (b) show the transmitted power (p.u.) and power angle (degrees). The transmitted power is $P = 1100$ MW,

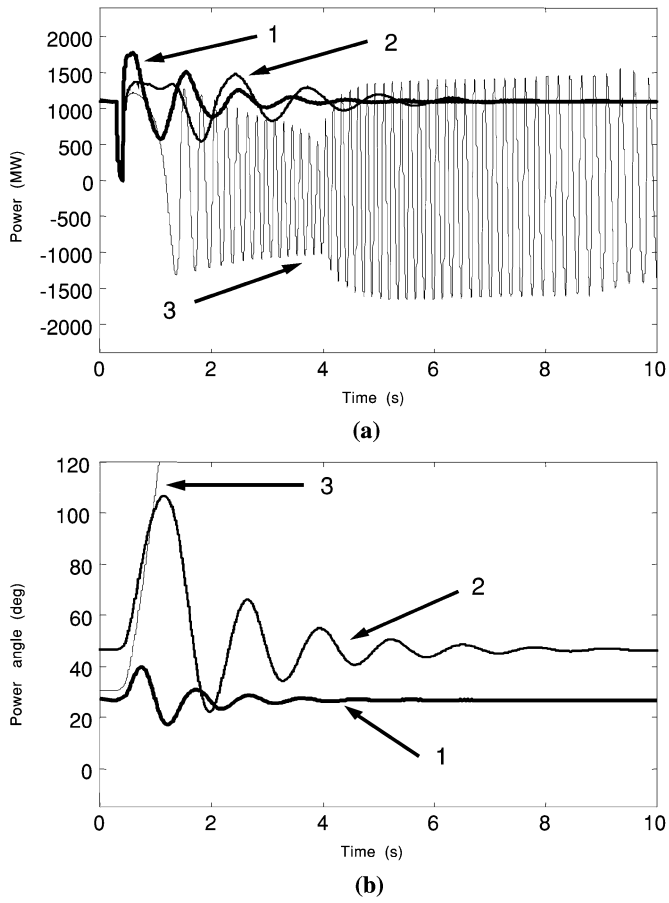


Fig. 11. System responses after a three-phase fault. (a) Transmitted power (MW). (b) Power angle (degrees). 1) Constant reactance mode $D_{\text{sssc}} = 0.7$. 2) Constant reactance mode $D_{\text{sssc}} = 0.5$. 3) Constant quadrature voltage mode $D_{\text{sssc}} = 0.7$.

which is greater than the maximum transient stability limit that is obtained with SSSC in constant quadrature voltage mode for $D_{\text{sssc}} = 0.7$. It is also the transient stability limit for $D_{\text{sssc}} = 0.5$ using the constant reactance mode. Curves 1 and 2 are for the constant reactance mode for $D_{\text{sssc}} = 0.7$ and 0.5, respectively. Curve 3 is for the constant quadrature voltage mode for $D_{\text{sssc}} = 0.7$. It can be seen from Fig. 11(b) that the generator remains in synchronism in curves 1 and 2, while in curve 3, the generator losses synchronism.

## VII. Discussion

The reason behind the difference in the performance of the SSSC in the two modes comes from the fact that in constant reactance mode, the SSSC voltage is function of the line current ($\overline{V_c} = -jX_{\text{sssc}}\overline{I_s}$) such that it emulates a series capacitor. Therefore, an increase in the voltage drop across the transmission line impedance ($jX_{\text{ex}}\overline{I_s}$), which resulted from increasing the transmitted power, is offset by the voltage of the SSSC $\overline{V_c}$. This can be seen in curve (1) in Figs. 5 and 6, when the damping power and the synchronizing power remain approximately constant as the transmitted power increases. However, in the constant quadrature voltage mode, the SSSC voltage is a constant quadrature voltage and independent of the line current ($\overline{V_c} = -jV_q$), and it acts as a constant reactive voltage compensator. In this situation, the SSSC cannot compensate for an increase in the voltage drop ($jX_{\text{ex}}\overline{I_s}$). As a result, the damping power and the synchronizing power drop as the transmitted power increases. This conclusion can be drawn from curve (2) in Figs. 5 and 6.

For the same reason, the transient stability limit of the system of Fig. 1 with SSSC in constant reactance mode is greater than the case when it is in constant quadrature voltage mode.

If the transient stability limit with SSSC operated in each mode without the damping controller is determined at different degrees of compensation, the same conclusion can be drawn [23]; that is, the transient stability limit with constant reactance mode is greater than the case with constant quadrature voltage mode. With the addition of the damping controller, the transient stability limit has been improved for both modes. The parameters of the damping controller (time constants $T_1, T_2, T_3$, and $T_4$ and the gain $K_d$), which have been used in this paper, were not optimum for both modes. The constant reactance mode was used to tune the parameters of the damping controller. The influence of the damping controller parameters on the transient stability limit obtained with each mode will be undertaken for further investigation.

## VIII. Conclusion

This paper has applied eigenvalue analysis and time-domain simulations to demonstrate the influence of the modes of operation of the SSSC on the small disturbance and transient stability of an SSSC-compensated radial power system. It has been shown that the SSSC operated in the constant reactance mode provides higher damping power, synchronizing power, and transient stability limit. Therefore, this mode reduces the size and consequently the cost of compensation by the SSSC.

## Appendix

A complete list of parameters used appears in the default options of HYPERSIM in the User's Manual [22].

1) Generator
   $S_B = 1700$ MV, $V_B = 315$ kV, $f_B = 60$ Hz, $r_a = 0, x_d = 1.8$ p.u., $x_l = 0.205$ p.u., $x_q = 1.77$ p.u., $x'_d = 0.293$ p.u., $x'_q = 0.438$ p.u., $x''_d = 0.244$ p.u., $x''_q = 0.244$ p.u., $T''_{\text{do}} = 5.5$ s, $T'_{\text{qo}} = 0.55$ s, $T''_{\text{do}} = 0.114$ s, $T''_{\text{qo}} = 0.21$ s.
2) Field Excitation System
   $K_a = 125, K_f = 0, K_p = 5.3, T_a = 0.001$ s, $T_f = 0, T_r = 0.02$ s, $V_{r\max} = 12.3$ p.u., $V_{r\min} = -5.7$ p.u.
3) Power System Stabilizer
   $K_{\text{ag}} = 1, K_{\text{ap}} = 1, K_s = 1, T_1 = 0.2$ s, $T_2 = 0.5$ s, $T_3 = 0.1$ s, $T_4 = 0.05$ s, $T_5 = 2$ s, $T_6 = 3$ s, $T_{\text{ag}} = 0, T_{\text{ap}} = 0.01$ s, $T_{w1} = T_{w2} = 0, V_{s\max} = 0.1$ p.u., $V_{s\min} = -0.1$ p.u.
4) Shaft
   $H_1 = 0.7988$ s, $H_2 = 1.2346$ s, $H_3 = 1.2118$ sec, $H_4 = 0.2202$ s, $D_1 = 0.000\,593\,38$ p.u., $D_2 = 0.0251$ p.u., $D_3 = 0.024\,62$ p.u., $D_4 = 0.0181$ p.u., $D_{12} = D_{23} = D_{34} = 0, K_{12} = 70.25$ p.u., $K_{23} = 51.36$ p.u., $K_{34} = 47.13$ p.u.
5) Turbine
   $T_3 = 0.3$ s, $T_4 = 0.5$ s, $T_5 = 1$ s, $T_6 = 1$ s, $T_7 = 1$

s, $T_{11} = 1$ p.u., $T_{12} = 1$ p.u., $T_{r1} = 5$ s, $T_{r2} = 0.3$ s, $T_{fh} = 0.55$ p.u., $T_{fi} = 0.225$ p.u., $T_{fl} = 0.225$ p.u., $T_{ai} = 1$ p.u., $T_{al} = 1$ p.u.,

6) Speed Governor System
$T_{\rm sw1} = 1, T_r = 0.045$ p.u., $T_{\rm db} = 0, T_{\rm pah1} = 0.25$ p.u., $T_{\rm pah2} = 0.25$ p.u., $T_{\rm ah\ lim} = 1.05$ p.u., $K_1 = 1$ p.u., $T_1 = 1.3$ s, $T_2 = 0.2$ s.

7) Boiler
$\rm ch\_press = 1.0$ p.u., $\rm ch\_b\,max = 1000$ p.u., $\rm ch\_kpc = 0.0001$ p.u., $\rm ch\_ki = 0.001$ p.u., $\rm ch\_k2 = 0.0001$ p.u., $\rm ch\_k3 = 0.001$ p.u., $\rm ch\_k4 = 1.0$ p.u., $\rm ch\_t8 = 1000$ s, $\rm ch\_t9 = 1000$ s, $\rm ch\_td = 0$ s.

8) Transformers
20 kV/315 kV, 24.45 kV/100 kV all in $\Delta/{\rm Y}-{\rm g}$ connection, $R_1 = 0.000\,19\ \Omega, L_1 = 0.000\,035\,3H, R_2 = 0.013\ \Omega, L_2 = 0.0024H$.

9) Transmission line
Length = 400 km, $r = 0.0147\ \Omega$/km, $l = 0.0009$ H/km, $c = 1.308{\rm e}-08$ F/km.

10) SSSC
$V_{\rm dcref} = 40$ kV, $C_{\rm dc} = 5000\ \mu$F.
DC Voltage Control: $K_p = 0.0009, K_i = 0.009$.
Damping Controller: $T_w = 10$ s, $T_1 = 0.1$ s, $T_2 = 0.0147$ s, $T_3 = 0.1$ s, $T_4 = 0.026$ s, $K_d = 0.3, V_{\rm dc\,max} = 4$ kv, $V_{\rm dc\,min} = -4$ kv.

## ACKNOWLEDGMENT

The author would like to thank Prof. L.-A. Dessaint, Prof. M. Lavoie, and Dr. R. Champagne for their friendship and assistance in the use of HYPERSIM.

## REFERENCES

[1] N. G. Hingorani, "A new scheme for subsynchronous resonance damping of torsional oscillations and transient torque," *IEEE Trans. Power App. Syst.*, vol. PAS-100, no. 4, pp. 1825–855, Apr. 1981.

[2] "CIGRE Paper, 38-02,", 1988.

[3] L. Gyugyi, "Solid-state control of AC power transmission," in *Proc. Int. Symp. Elect. Energy Convers. Power Syst.*, Paper no. T-IP.4, Capri, Italy, 1989.

[4] L. Gyugyi, C. D. Schauder, and K. K. Sen, "Static synchronous series compensator: A solid-state approach to the series compensation of transmission lines," *IEEE Trans. Power Del.*, vol. 12, no. 1, pp. 406–417, Jan. 1997.

[5] K. K. Sen, "SSSC-static synchronous series compensator: Theory, modeling, and applications," *IEEE Trans. Power Del.*, vol. 13, no. 1, pp. 241–246, Jan. 1998.

[6] X. Wang, S.-Z. Dai, and B.-T. Ooi, "A series capacitive reactance compensator based on voltage source PWM converter," in *Proc. IEEE IAS Ann. Meeting*, 1991, pp. 918–924.

[7] B. T. Ooi, S. Z. Dai, and X. Wang, "Solid state series capacitive reactance compensator," *IEEE Trans. Power Del.*, vol. 7, no. 2, pp. 914–919, Apr. 1992.

[8] B. T. Ooi and S. Z. Dai, "Series type solid state static VAR compensator," *IEEE Trans. Power Electron.*, vol. 8, no. 2, pp. 164–169, Mar. 1993.

[9] R. G. Harley, B. S. Rigby, and G. D. Jennings, "Design of a controlled converter which emulates a series capacitive compensator for long power lines," in *Proc. Int. Conf. Power Electron. Motion Control*, Warsaw, Poland, Sep. 1994, pp. 213–218.

[10] F. A. L. Jowder and B. T. Ooi, "Series compensation of a radial power system by a combination of SSSC and dielectric capacitor," *IEEE Trans. Power Del.*, vol. 20, no. 1, pp. 458–465, Jan. 2005, to be published.

[11] R. M. Mathur and R. K. Varma, *Thyristor-Based FACTS Controllers for Electrical Transmission Systems*, 1st ed. Piscataway, NJ: IEEE Press, 2002, p. 345.

[12] E. Larsen, C. Bowler, B. Damsky, and S. Nilsson, "Benefits of Thyristor-Controlled Series Compensation," CIGRE, Paris, France, 1992. Paper 14/37/38-04.

[13] C. Gama and R. Tenorio, "Improvements for power system performance: Modeling, analysis, and benefits of TCSC," in *Proc. Power Eng. Soc. Winter Meeting*, Singapore, Jan. 2000.

[14] S. Nyati, C. A. Wenger, R. W. Delmerico, R. J. Piwko, D. H. Baker, and A. Edris, "Effectiveness of thyristor-controlled series capacitor in enhancing power system dynamics: An analog simulator study," *IEEE Trans. Power Del.*, vol. 9, no. 2, pp. 1018–1027, Apr. 1994.

[15] L. Angquist, G. Ingestrom, and H. A. Jonsson, "Dynamical performance of TCSC schemes," CIGRE Paper 14-302, Paris, France, 1996.

[16] C. Gama and M. Noroozian, "Control strategy for damping power swings using TCSC," in *Proc. CIGRE Symp.*, Kuala Lumpur, Malaysia, 1999.

[17] M. Noroozian, M. Ghandhari, G. Andersson, J. Gronquist, and I. Hiskens, "A robust control strategy for shunt and series reactive compensators to damp electromechanical oscillations," *IEEE Trans. Power Del.*, vol. 16, no. 4, pp. 812–817, Oct. 2001.

[18] N. Martins, H. Pinto, and J. Paserba, "Using a TCSC for power scheduling and system oscillations damping-small signal and transient stability studies," in *Proc. Power Eng. Soc. Winter Meeting*, Singapore, Jan. 2000, pp. 1455–1461.

[19] A. Mehraban, A. Edris, C. Schauder, and J. H. Provanzana, "Installation, commissioning, and operation of the world's first UPFC on the AEP system," in *Proc. Int. Conf. Power Syst. Technol.*, vol. 1, Aug. 1998, pp. 323–327.

[20] F. J. Swift and H. F. Wang, "Applications of the controllable series compensator in damping power system oscillations stability," *Proc. Inst. Elect. Eng.—Gen., Transm., Distrib.*, vol. 143, no. 4, pp. 359–364, Jul. 1996.

[21] B. S. Rigby, N. S. Chonco, and R. G. Harley, "Application and analysis of power oscillation damping scheme using a voltage source inverter," *IEEE Trans. Ind. Appl.*, vol. 38, no. 4, pp. 1105–1113, Jul./Aug. 2002.

[22] *Power System Simulator-HYPERSIM: User's Manual*, Jun. 1999. DMNU-57 001-1.3A, TEQSIM International, Inc..

[23] F. A. L. Jowder, "Embedded SSSC in Series Capacitor Compensation and in Voltage-Source Converter," Ph.D. dissertation, McGill Univ., Montreal, QC, Canada, 2004.

[24] P. Kundur, *Power System Stability and Control*. New York: McGraw-Hill, 1994.

**Fawzi A. L. Jowder** (M'99) was born in Muharraq, Bahrain, in 1971. He received the B.Sc. degree with distinction from the University of Bahrain, Isa Town, Bahrain, in 1996, the M.Sc. degree with distinction from the University of Manchester Institute of Science and Technology (UMIST), Manchester, U.K. in 1999, and the Ph.D. degree from McGill University, Montreal, QC, Canada in 2004, all in electrical engineering.

He is presently an Assistant Professor with the Department of Electrical and Electronic Engineering at the University of Bahrain. His interests include FACTS, HVDC, dispersed generation, and electrical machines modeling.